Risk of misinterpretation of low-spin non-yrast bands as wobbling bands

S. Guo,[1,2] X. H. Zhou,[1,2,*] C. M. Petrache,[3] E. A. Lawrie,[4,5] S. Mthembu,[4,5] Y. D. Fang,[1,2] H. Y. Wu,[6] H. L. Wang,[7] H. Y. Meng,[7] G. S. Li,[1,2] Y. H. Qiang,[1] J. G. Wang,[1,2] M. L. Liu,[1,2] Y. Zheng,[1,2] B. Ding,[1,2] W. Q. Zhang,[1,2] A. Rohilla,[1] K. R. Mukhi,[1] Y. Y. Yang,[1,2] H. J. Ong,[1,2] J. B. Ma,[1,2] S. W. Xu,[1,2] Z. Bai,[1,2] H. L. Fan,[8] J. F. Huang,[9] J. H. Li,[1] J. H. Xu,[1] B.F. Lv,[1] W. Hua,[10] Z. G. Gan,[1,2] and Y. H. Zhang[1,2]

[1] *CAS Key Laboratory of High Precision Nuclear Spectroscopy, Institute of Modern Physics, Chinese Academy of Sciences, Lanzhou 730000, China*
[2] *School of Nuclear Science and Technology, University of Chinese Academy of Science, Beijing 100049, People's Republic of China*
[3] *Université Paris-Saclay, CNRS/IN2P3, IJCLab, 91405 Orsay, France*
[4] *iThemba LABS, National Research Foundation, PO Box 722, 7131 Somerset West, South Africa*
[5] *Department of Physics & Astronomy, University of the Western Cape, P/B X17, Bellville ZA-7535, South Africa*
[6] *State Key Laboratory of Nuclear Physics and Technology, School of Physics, Peking University, Beijing 100871, China*
[7] *School of Physics and Microelectronics, Zhengzhou University, Zhengzhou 450001, China*
[8] *College of Engineering Physics, Shenzhen Technology University, Shenzhen 518118, China*
[9] *Guangzhou Municipal Ecological Environment Bureau Huadu District Branch, Guangzhou 510800, People's Republic of China*
[10] *Sino-French Institute of Nuclear Engineering and Technology, Sun Yat-Sen University, Zhuhai 519082, China*

(Dated:)

It is argued that the experimental criteria recently used to assign wobbling nature to low-spin bands in several nuclei are insufficient and risky. New experimental data involving angular distribution and linear polarization measurements on an excited band in ^{187}Au, previously interpreted as longitudinal wobbling, are presented. The new data show that the linking transitions have dominant magnetic nature and exclude the wobbling interpretation.

PACS numbers: 21.10.Re, 21.60.Ev, 23.20.Lv, 27.60.+j

Although the atomic nucleus is a complicated quantum many-body system, its motion often resembles that of a simple physical system in the macroscopic world. Half a century ago it was predicted, based on the Unified Model, that similar to the precession of a gyroscope in classical mechanics wobbling motion exists in triaxial nuclei [1]. When the nucleus wobbles the principle nuclear axis having the largest moment of inertia plays the role of the axle of a gyroscope, and rotates around the space-fixed angular momentum. Nuclear wobbling was first identified two decades ago, when a series of wobbling bands called triaxial superdeformed (TSD) bands, were observed in several nuclei of the 160 mass region [2–7].

Recently, following the introduction of longitudinal and transverse wobbling by Frauendorf and Dönau [8], new cases of low-spin wobbling bands have been reported. This new interpretation describes a system based on a rotating triaxial core coupled to an odd quasiparticle, assuming that the moments of inertia of the triaxial core are of hydrodynamic type and the angular momentum of the odd quasiparticle is rigidly aligned with one of the principal axes (frozen approximation). Angular momentum coupling of longitudinal (transverse) type is formed where the quasiparticle angular momentum is oriented parallel (perpendicular) to the rotational axis with the largest moment of inertia. The wobbling equations approximate the unfavoured rotation of a triaxial nucleus as an excitation of wobbling phonons. They furnish an explanation of the observed decreasing trend of the relative excitation energy of the yrare band (wobbling frequency) in some nuclei as resulting from the proposed transverse wobbling, while for simple wobbler or for longitudinal wobbling the wobbling frequency increases. Later a debate about the validity of this picture followed mainly because the effect of the Coriolis force on the odd nucleon in the transverse coupling is neglected in the frozen transverse approximation [9–11]. All recently reported low-spin wobbling bands were interpreted using this approximation, for instance, several excited bands in ^{135}Pr, ^{105}Pd, and ^{183}Au were interpreted as transverse wobbling [12–15], while the yrare bands in ^{133}La, ^{187}Au, and ^{127}Xe were considered as longitudinal wobbling [16–18].

These low-spin wobbling bands are estimated to correspond to smaller quadrupole deformation and softer gamma deformation comparing to the high-spin wobbling bands in 160 mass region [19], extending the frontier of collective excitation. It is worthwhile to critically assess the evidence supporting such an interpretation. Up to now, the behaviours of all the reported wobbling bands are found similar with those of the unfavoured signature partners of low-Ω rotation aligned configurations, except for the predominantly $E2$ character of the Δ I=1 transitions linking the yrare to the yrast bands. Therefore, the deduced large $E2/M1$ mixing ratios ($|\delta| > 1$) is considered as the key experimental criterion for a wobbling assignment. It is worth noting that the large mixing ratios of the connecting transitions are only a necessary,

but not a sufficient condition for wobbling motion, since they cannot exclude some other possible collective modes, such as tilted precession [20]. In any case for a confident identification of a wobbling band the alternative possibility where the band is linked to the yrast band by $M1$ dominated transitions (with small mixing ratios) should be firmly excluded. For all the reported low-spin wobbling bands, the mixing ratios were deduced from angular distribution and/or linear polarization measurements.

Angular distribution curves can be calculated assuming appropriate values for the mixing ratio (δ) and the alignment parameter (σ/I). It is possible to deduce suitable mixing ratios with correspond to good agreements between the calculated curves and the experimental results. Usually, two similar curves with two mixing ratios $|\delta_1| > 1$ and $|\delta_2| < 1$ match the experimental data well (see Fig. 1). Therefore, one should first find both δ_1 and δ_2 solutions by fitting the experimental points, and then plot the two curves together, in comparison with the experimental results. The angular distribution curve should pass through most of the experimental data (including their uncertainties), then the corresponding δ can be considered as a possible solution. Mixing ratios for the linking transitions of the wobbling bands, extracted from angular distribution measurements have been reported in ^{135}Pr [12, 13], ^{133}La [16] and ^{187}Au [17]. However, in all those works, the curves for $|\delta_2| < 1$ were not shown, while those for $|\delta_1| > 1$ were only compared with curves for pure $M1$ transitions ($\delta = 0$). This could create a false belief that the correct solution for the mixing ratio is reliably established. Actually, both δ_1 and δ_2 can be possible solutions for the two works on ^{135}Pr (see Figs. 1a, 1b) [12] and ^{133}La (see Figs. 1g, 1h) [16]. For the other two works (see Fig. 1 c-f) [13, 17], the reported errors are so small that even the reported curves do not pass through the uncertainty regions of the majority of the data points. It has not yet been demonstrated how to restrict the uncertainty to a negligible level, especially taking into account comparisons with previous works performed using similar experimental setups and statistics [12].

For the angular distribution measurements, sometimes a preferable mixing ratio is suggested based on the χ^2 fitting. The χ^2 value is useful to evaluate a fit on directly measurable experimental results. However, the counts for angular distribution analysis are not peak areas measured directly, but deduced from γ-γ matrices based on a large number of independent events. The results, especially the central values can be influenced by the choice of the parameters used in gating and fitting the peak areas. Usually such influence should be well evaluated and included in the error. However, the deviations on central values cannot be fixed back, leading to the sensitivity of the χ^2 value on the selection of those parameters. Therefore it cannot be taken as a decisive criterion, in particular if unreasonably small error bars are presented

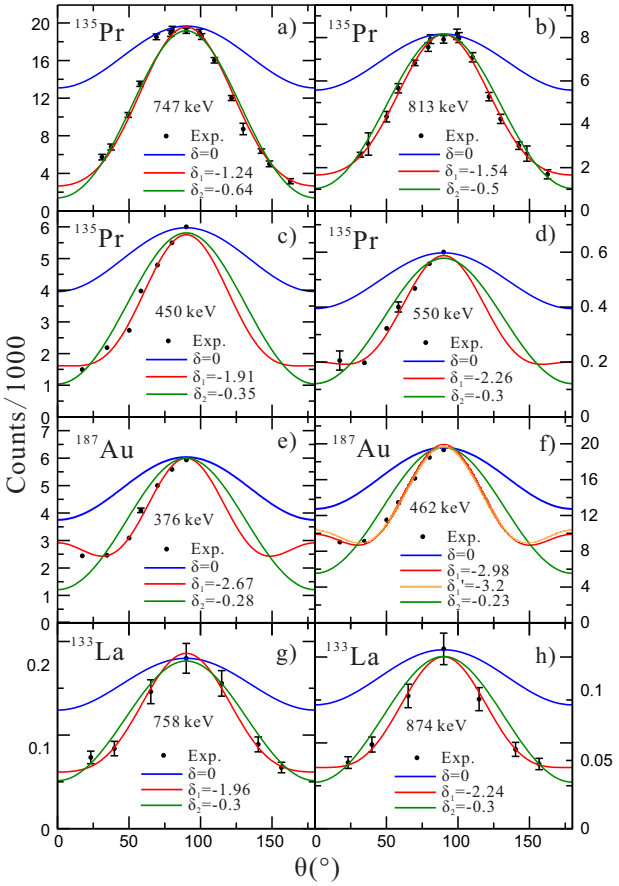

FIG. 1. Estimated angular distribution curves and experimental results for the reported transverse wobbling bands in ^{135}Pr, and longitudinal wobbling bands in ^{187}Au and ^{133}La. The curves for pure $M1$ transition (in blue) and large δ (in red) are taken from the original figures in Refs. [12, 13, 16, 17], and those with smaller mixing ratios and same σ/I are also plotted (in green) for comparison. For the 462-keV transition in ^{187}Au, δ = -2.98 is deduced from the curve marked with δ = -3.2 in Ref. [17], therefore both curves are plotted.

without details.

Their central values can be influenced in certain ranges due to the artificial selection of the parameters used in gating and fitting the peak areas. Therefore the χ^2 value is sensitive to artificial factors, and is less reliable for angular distribution measurements, especially when a convincing analysis on the induced uncertainty is absent.

Linear polarization measurements were carried out for ^{135}Pr [12], ^{105}Pd [14], ^{133}La [16], ^{183}Au [15] and ^{127}Xe [18]. A series of parameters, such as the asymmetry correction (a), the polarization sensitivity (Q), and σ/I, should be rigorously calibrated or evaluated to deduce convincing polarization values [21]. However, these essential parameters are not reported for all these works, except the calibration of a reported in a corresponding PhD thesis on ^{135}Pr [22]. Furthermore, the gated spectra for polarization analysis and corresponding arguments

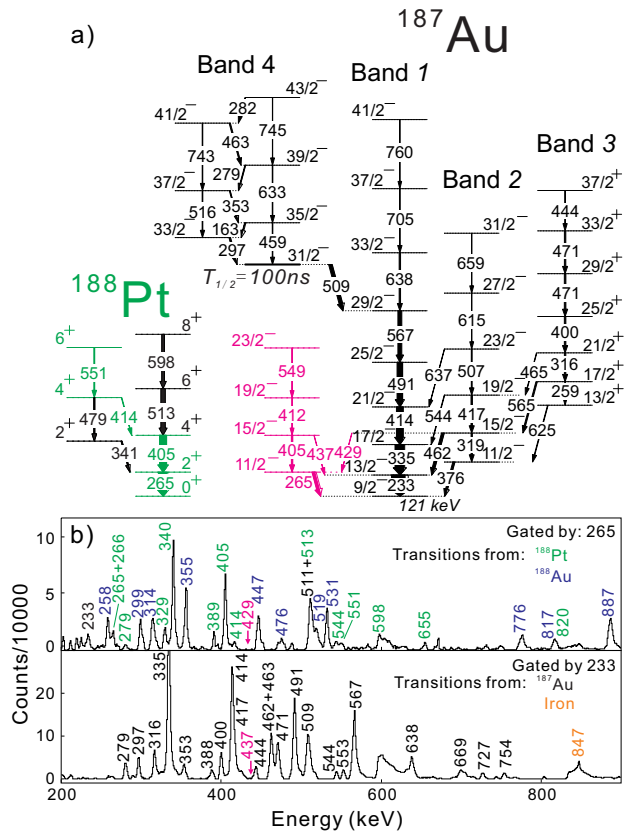

FIG. 2. a) Partial level scheme of ^{187}Au and ^{188}Pt. The structure in red was reported in Ref. [17], but not confirmed in the present work. Instead, a sequence in green is found with similar energies which belongs to ^{188}Pt. b) Typical spectra gated by the 265- and 233-keV transitions.

on gating transition selections were also absent for most of those works. Hardly can the experimental results be assessed with all the mentioned information absent for ^{105}Pd and ^{127}Xe. Nevertheless, with limited information reported, severe problems have been found in the experimental results on ^{135}Pr [23], ^{133}La [24] and ^{183}Au [25], which sheds doubts on the assigned wobbling nature to the bands.

Among the reported low-spin wobbling bands, the interpretation for that in ^{187}Au is most intriguing. To achieve the geometry of the claimed longitudinal wobbling, the quasiproton should be located in the middle of a j-shell [17], while the proton Fermi surface is close to the bottom of the intruder $h_{9/2}$ sub-shell [26]. In addition, the large mixing ratios were deduced only from angular distribution measurements, with extremely small errors, while essential experimental information previously published on conversion coefficients from the β-decay of the $T_{1/2}$=2.4 min, J^{π}=13/2$^+$ high-j isomer in ^{187}Hg was not mentioned [27, 28].

In order to clarify the existing contradictory experimental information and to further investigate the nature of the yrare band in ^{187}Au, an experiment has been carried out at the Heavy Ion Research Facility in Lanzhou (HIRFL) [29, 30], China. The excited states of ^{187}Au were studied using the ^{175}Lu(^{18}O,6n) reaction with a 108-MeV ^{18}O beam and a stack of two self-supported natural Lu targets with a thickness of 0.7 mg/cm^2 each. The γ rays were detected by a detector array consisting of 8 segmented clover detectors and 16 coaxial High-purity germanium (HPGe) detectors. Eight of the HPGe detectors were equipped with anti-Compton shields. All clover detectors were placed in a ring perpendicular to the beam direction. The 16 HPGe detectors were placed in four rings at 26°, 51°, 129° and 154°. Approximately 5×10^{10} double- or higher-fold events have been recorded by a general-purpose digital data acquisition system [31].

Fig. 2a shows a partial level scheme of ^{187}Au obtained in the present work, together with a partial level scheme of ^{188}Pt. The structure in red was reported in Ref. [17], and interpreted as the unfavored signature branch of the $\pi h_{9/2}$ band (band 1) in ^{187}Au. However, the sequence including the 265-, 405-, 412, and 549-keV transitions have very similar energies to the 265-, 405-, 414-, 551-keV transitions in the ground state band and the γ band in ^{188}Pt [32] (the sequence in green in Fig. 2a). Our data shows no sign of the previously proposed linking transitions of 429 keV and 437 keV, (see for instance the spectra gated by the transitions below in Fig. 2b). Therefore, the present work does not support the existence of such a band in ^{187}Au. In fact, from a detailed study of ^{187}Hg β-decay by Rupnik et al. [28], this structure was also absent, while all the states and transitions below 19/2$\hbar$ in bands 2 and 3 have been observed.

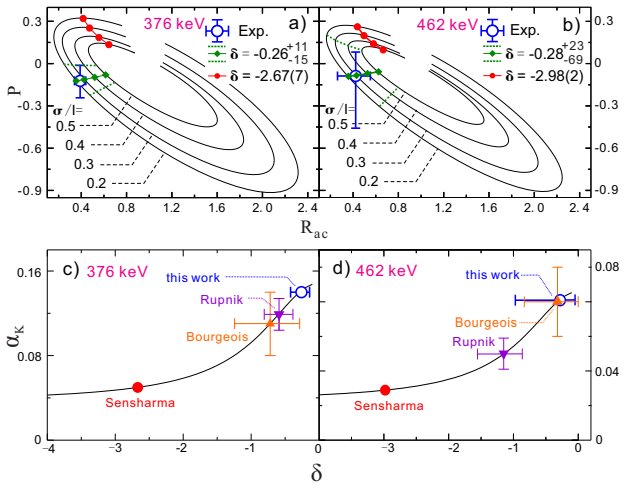

FIG. 3. a & b, Plots for polarization versus R_{ac} as a function of mixing ratios with different σ/I parameters, together with experimental results and estimated results for certain mixing ratios. c & d, Internal conversion coefficients as a function of mixing ratios, together with the experimental results from the present work and those from Bourgeois, *et al.* [27], Rupnik, *et al.* [28] and Sensharma, *et al.* [17].

TABLE I. Energies of transitions (E_γ), spin and parities of initial and final states ($I_i^\pi \to I_f^\pi$), angular correlation ratios (R_{ac}), linear polarization coefficients (P), $E2/M1$ mixing ratios (δ) for three linking transitions between bands 1 and 2 in ^{187}Au, and the reduced transition probability ratios between these transitions and inband $E2$ transitions depopulating the same states.

E_γ(keV)	$I_i^\pi \to I_f^\pi$	R_{ac}	P	δ	B(M1)$_{out}$/B(E2)$_{in}$	B(E2)$_{out}$/B(E2)$_{in}$
376	$11/2^- \to 9/2^-$	0.39(5)	-0.12^{+11}_{-12}	-0.26^{+11}_{-16}		
462	$15/2^- \to 13/2^-$	0.42^{+13}_{-16}	-0.09^{+17}_{-37}	-0.28^{+23}_{-69}	0.045^{+9}_{-23}	0.024^{+152}_{-23}
544	$19/2^- \to 17/2^-$			-0.4^{+4}_{-21} [a]	0.016^{+2}_{-14}	0.012^{+63}_{-12}

a) Deduced from the internal conversion coefficients reported in Ref. [28]

The mixing ratios of the transitions linking band 2 to band 1 reported in the present work are deduced using two complementary measurements of a two-point angular-correlation ratio, R$_{ac}$, and of linear polarization, P. R$_{ac}$ was deduced from the ratio of the γ-ray intensities measured in the spectra of the 26° and 90° detectors, gated on transitions observed in all detectors. The linear polarization, P, was deduced based on the Compton scattering events in two adjacent crystals of the clover detectors. The supplementary material provides more experimental details [19]. Table I summarizes the measured values of R$_{ac}$ and P for the linking transitions between bands 2 and 1. The measured polarization of the 376-keV transition is in good agreement with the value of -0.10(5) reported earlier [26]. The mixing ratios were deduced from the measured values of R$_{ac}$ and P using the ellipse-like curves calculated as a function of δ, shown in Fig. 3. The curves are sensitive to the σ/I parameter, which can be affected by states with lifetimes of the order of a picosecond or larger which are usually present in the low-spin region. The δ values are deduced with the σ/I parameter not restricted. Despite the large error bars it is clear that the absolute values of the deduced mixing ratios are smaller than 1 confirming the dominant $M1$ nature of these transitions. Data points that correspond to the large mixing ratios deduced in Ref. [17] are shown in red in Fig. 3. They are in distinct disagreement with both the presently deduced values and with the values obtained from previous internal conversion coefficients measurements [27, 28] (see Fig. 3).

The experimentally measured reduced transition probability ratios $B(E2)_{out}/B(E2)_{in}$ extracted from the present data are listed in Table I. Taking into account the low values of these ratios and that $B(E2)_{in}$ values in the collective bands of ^{187}Au are expected to be ≈ 100 - 200 W.u. [33, 34], the expected values of $B(E2)_{out}$ are only a few W.u., which is inconsistent with wobbling and in general does not support collective type of excitation.

In order to study further the nature of band 2, one-quasiparticle-plus-triaxial-rotor (QTR) model calculations using the codes of P. Semmes and I. Ragnarsson [35] were carried out (for more details see the supplementary material [19]). Standard parameters are used for the Nilsson potential [36] and for the pairing strength. The moments of inertia of the core have irrotational-flow nature, as suggested by an empirical evaluation [37]. The spin dependence is taken into account by assuming variable moments of inertia described by the Harris parameters $J_0 = 25\ \hbar^2\text{MeV}^{-1}$ and $J_1 = 8\ \hbar^4\ \text{MeV}^{-3}$. The adopted quadrupole deformation of $\varepsilon = 0.21$ is similar to that previously used in Refs. [17, 28]. The adopted triaxial deformation is $\gamma = 12°$, as found in the theoretical calculations for ^{186}Pt [38]. The calculated proton Fermi level is near the highest $h_{11/2}$ and lowest $h_{9/2}$ orbitals, as in Ref. [26]. The 9 negative-parity orbitals closest to the Fermi level are included in the calculations.

The calculated excitation energies of the two lowest-energy rotational bands with $h_{9/2}$ nature are shown in Fig. 4. The yrast and yrare bands are based on dominant single-particle contribution from the lowest-energy and the second-lowest energy $h_{9/2}$ orbitals, respectively, suggesting that the excitation between the two bands is dominated by non-collective mechanism. The calculated mixing ratios and $B(E2)_{out}/B(E2)_{in}$ ratios are in good agreement with our data and with data from Refs. [26–28], but in contrast with the data from Ref. [17] (see

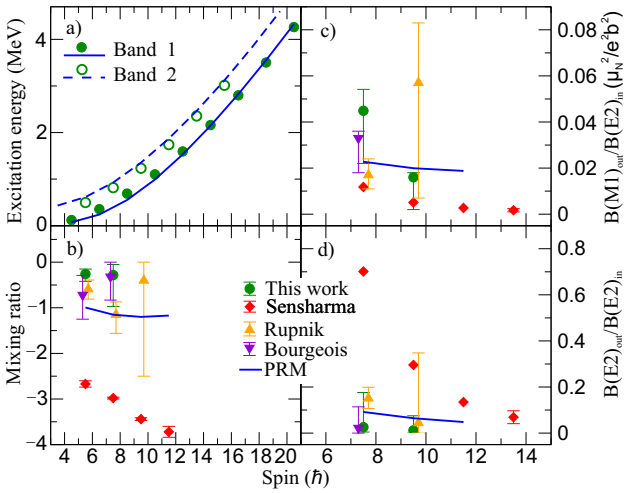

FIG. 4. Experimental and theoretical results for the excitation energies (a), mixing ratios (b), $B(M1)_{out}/B(E2)_{in}$ ratios (c) and $B(E2)_{out}/B(E2)_{in}$ ratios (d) for bands 1 and 2 of ^{187}Au. The values of previously measured mixing ratios [17, 26–28], are also shown.

Fig. 4b), further supporting the proposed non-collective character of the excitation.

In summary, the recently reported longitudinal wobbling band in ^{187}Au is re-investigated via an experiment involving angular distribution and linear polarization measurements. The deduced low mixing ratios for the linking transitions between the yrare and the yrast bands are in disagreement with the high values reported by Sensharma et al. [17], but in agreement with the conversion coefficients reported by Bourgeois et al. [27] and Rupnik et al. [28], and with the linear polarization value reported by Bourgeois et al. [26]. These mixing ratios indicate low $B(E2)_{out}/B(E2)_{in}$ ratios and show that the yrare band is not excited from the yrast band by a predominantly collective excitation, ruling out the longitudinal wobbling interpretation proposed in Ref. [17]. This conclusion is further supported by the QTR-model calculations which reproduce well the experimental data.

The risk of misinterpretation of yrare bands as due to wobbling motion is also highlighted by the concerns about the mixing ratio measurements in ^{135}Pr [23], ^{133}La [24], and ^{183}Au [25], putting forward the need to re-measure the mixing ratios for other candidate wobbling bands too. Furthermore, the large mixing ratios are indicative of collective excitation, but not necessarily of wobbling motion, which requires the observation of quantization in the excitation energies and reduced transition probabilities, as a basic feature of all phonon excitations. More experimental and theoretical works are needed to clarify the nature of the low-spin yrare bands.

The authors would like to thank the accelerator crew of HIRFL for providing the stable ^{18}O beam during the pandemic of COVID-19. This work has been supported by the Strategic Priority Research Program of Chinese Academy of Sciences, (Grant No. XDB34000000), the National Key R&D Program of China (Contract Nos. 2018YFA0404402 and 2018YFA0404400), the Key Research Program of the Chinese Academy of Sciences (Grant No. XDPB09-02), the National Natural Science Foundation of China (Grant Nos. U1932137, U1732139, U1832134, 11775274, 11975209, and 11805289), the Cai YuanPei 2018 Project No. 41458XH, and the National Research Foundation of South Africa, GUN: 93531, 109134.

* *Corresponding author*; zxh@impcas.ac.cn

[1] A. Bohr and B. R. Mottelson, **Nuclear Structure (Benjamin, New York, 1975), Vol. II.** (1975).
[2] S. W. Ødegård, G. B. Hagemann, D. R. Jensen, M. Bergström, B. Herskind, and G. Sletten *et al.*, Phys. Rev. Lett. **86**, 5866 (2001).
[3] D. R. Jensen, G. B. Hagemann, I. Hamamoto, S. W. Ødegård, B. Herskind, and G. Sletten *et al.*, Phys. Rev. Lett. **89**, 142503 (2002).
[4] P. Bringel, G. B. Hagemann, H. Hübel, A. Al-khatib, P. Bednarczyk, and A. Bürger *et al.*, The European Physical Journal A - Hadrons and Nuclei **24**, 167 (2005).
[5] G. Schönwaβer, H. Hübel, G. Hagemann, P. Bednarczyk, G. Benzoni, and A. Bracco *et al.*, Physics Letters B **552**, 9 (2003).
[6] H. Amro, W. Ma, G. Hagemann, R. Diamond, J. Domscheit, and P. Fallon *et al.*, Physics Letters B **553**, 197 (2003).
[7] D. J. Hartley, R. V. F. Janssens, L. L. Riedinger, M. A. Riley, A. Aguilar, and M. P. Carpenter *et al.*, Phys. Rev. C **80**, 041304(R) (2009).
[8] S. Frauendorf and F. Dönau, Phys. Rev. C **89**, 014322 (2014).
[9] K. Tanabe and K. Sugawara-Tanabe, Phys. Rev. C **95**, 064315 (2017).
[10] S. Frauendorf, Phys. Rev. C **97**, 069801 (2018).
[11] K. Tanabe and K. Sugawara-Tanabe, Phys. Rev. C **97**, 069802 (2018).
[12] J. T. Matta, U. Garg, W. Li, S. Frauendorf, A. D. Ayangeakaa, and D. Patel *et al.*, Phys. Rev. Lett. **114**, 082501 (2015).
[13] N. Sensharma, U. Garg, S. Zhu, A. Ayangeakaa, S. Frauendorf, and W. Li *et al.*, Physics Letters B **792**, 170 (2019).
[14] J. Timár, Q. B. Chen, B. Kruzsicz, D. Sohler, I. Kuti, and S. Q. Zhang *et al.*, Phys. Rev. Lett. **122**, 062501 (2019).
[15] S. Nandi, G. Mukherjee, Q. B. Chen, S. Frauendorf, R. Banik, and S. Bhattacharya *et al.*, Phys. Rev. Lett. **125**, 132501 (2020).
[16] S. Biswas, R. Palit, S. Frauendorf, U. Garg, W. Li, and G. H. Bhat *et al.*, The European Physical Journal A **55**, 159 (2019).
[17] N. Sensharma, U. Garg, Q. B. Chen, S. Frauendorf, D. P. Burdette, and J. L. Cozzi *et al.*, Phys. Rev. Lett. **124**, 052501 (2020).
[18] S. Chakraborty, H. Sharma, S. Tiwary, C. Majumder, A. Gupta, and P. Banerjee *et al.*, Physics Letters B **811**, 135854 (2020).
[19] See Supplementary Material for more details.
[20] E. A. Lawrie, O. Shirinda, and C. M. Petrache, Phys. Rev. C **101**, 034306 (2020).
[21] K. Starosta, T. Morek, C. Droste, S. Rohoziński, J. Srebrny, and A. Wierzchucka *et al.*, Nucl. Instrum. Methods Phys. Res., Sect. A **423**, 16 (1999).
[22] J. T. Matta, Springer Theses **ph.D thesis**.
[23] S. Guo, C. Petrache, to be published, arXiv **2011**, 14364 (2020).
[24] W. Hua, S. Guo, C. Petrache, to be published, arXiv **2011**, 14369 (2020).
[25] S. Guo, C. Petrache, to be published, arXiv **2012**, 00343 (2020).
[26] C. Bourgeois, M. G. Porquet, N. Perrin, H. Sergolle, F. Hannachi, G. Bastin, and F. Beck, Zeitschrift für Physik A Atomic Nuclei **333**, 5 (1989).
[27] C. Bourgeois, P. Kilcher, J. Letessier, V. Berg, and M. Desthuilliers, Nuclear Physics A **295**, 424 (1978).
[28] D. Rupnik, E. F. Zganjar, J. L. Wood, P. B. Semmes, and P. F. Mantica, Phys. Rev. C **58**, 771 (1998).
[29] J. Xia, W. Zhan, B. Wei, Y. Yuan, M. Song, and W. Zhang *et al.*, Nucl. Instrum. Methods Phys. Res., Sect. A **488**, 11 (2002).
[30] Z. Sun, W.-L. Zhan, Z.-Y. Guo, G. Xiao, and J.-X. Li,

Nucl. Instrum. Methods Phys. Res., Sect. A **503**, 496 (2003).
[31] H. Wu, Z. Li, H. Tan, H. Hua, J. Li, and W. Hennig *et al.*, Nucl. Instrum. Methods Phys. Res., Sect. A **975**, 164200 (2020).
[32] S. Mukhopadhyay, D. C. Biswas, S. K. Tandel, S. Frauendorf, L. S. Danu, and P. N. Prashanth *et al.*, Phys. Rev. C **96**, 014315 (2017).
[33] C. M. BAGLIN, Nuclear Data Sheets **99**, 1 (2003).
[34] M. Basunia, Nuclear Data Sheets **110**, 999 (2009).
[35] P. B. Semmes and I. Ragnarsson, in *Proceedings of the International Conference on High-Spin Physics and Gamma-Soft Nuclei, Pittsburg, 1990*, edited by J. X. Saladin, R. A. Sorenson, and C.M.Vincent (World Scientific, Singapore, 1991), p. 500; in *Future Directions in Nuclear Physics with 4π Gamma Detection Systems of the New Generation*, edited by J. Dudek and B. Haas (AIP Conf. Proc. 259, 1992), p. 566.
[36] T. Bengtsson and I. Ragnarsson, Nuclear Physics A **436**, 14 (1985).
[37] J. Allmond and J. Wood, Physics Letters B **767**, 226 (2017).
[38] R. Rodríguez-Guzmán, P. Sarriguren, L. M. Robledo, and J. E. García-Ramos, Phys. Rev. C **81**, 024310 (2010).